Band-dependent Quasiparticle Dynamics in Single Crystals of the $Ba_{0.6}K_{0.4}Fe_2As_2$ Superconductor Revealed by Pump-Probe Spectroscopy

Darius H. Torchinsky,[1] G. F. Chen,[2] J. L. Luo,[2] N. L. Wang,[2] and Nuh Gedik[1,*]

[1]*Department of Physics, Massachusetts Institute of Technology, Cambridge, Massachusetts, 02139, USA*
[2]*Beijing National Laboratory for Condensed Matter Physics, Institute of Physics, Chinese Academy of Sciences, Beijing 100190, China*

We report on band-dependent quasiparticle dynamics in $Ba_{0.6}K_{0.4}Fe_2As_2$ ($T_c = 37$ K) measured using ultrafast pump-probe spectroscopy. In the superconducting state, we observe two distinct relaxation processes: a fast component whose decay rate increases linearly with excitation density and a slow component with an excitation density independent decay rate. We argue that these two components reflect the recombination of quasiparticles in the two hole bands through intraband and interband processes. We also find that the thermal recombination rate of quasiparticles increases quadratically with temperature. The temperature and excitation density dependence of the decays indicates fully gapped hole bands and nodal or very anisotropic electron bands.

One of the main factors complicating studies of the iron pnictides is the existence of multiple electron and hole bands crossing the Fermi surface [1–3], each of which develops a gap upon cooling below the superconducting transition temperature T_c. Consequently, there is still no consensus within the community concerning the symmetry and structure of the superconducting order parameter. Angle resolved photoemission spectroscopy (ARPES) measurements consistently show nearly isotropic gaps with no evidence of nodes [1], although the surface-selective nature of ARPES, and its diminished resolution at the Brillouin zone corner may obscure the presence of nodes. Meanwhile, many bulk measurements which integrate across the Brillouin zone have painted a somewhat different picture; nuclear magnetic resonance (NMR) spin relaxation measurements of the $1/T_1$ relaxation rate [4] and penetration depth experiments [5] both yield a power law temperature dependence usually associated with nodes.

Theoretical approaches also suggest a number of different pairing symmetries both with and without nodes. Mazin *et al.* proposed a nodeless extended *s*-wave gap that changes sign between the electron and hole pockets ($s_{\pm}$) [2], Graser *et al.* found $s_{\pm}$ pairing symmetry with nodes on the electron pockets or $d_{x^2-y^2}$ with nodes on the hole pockets, depending upon the doping [6] while Yanagi and co-workers proposed a d_{xy} state with nodes on both the electron and hole pockets [7]. These different scenarios arise as a result of the interplay between intra and interband interactions [8]. It is therefore of crucial importance to be able to experimentally probe the low energy excitations of these materials in a band-sensitive manner in order to better elucidate the superconducting order parameter.

Time resolved optical pump-probe spectroscopy [9–14] is a powerful, bulk-sensitive technique which provides a unique window upon quasiparticle (QP) interactions in the iron pnictides. In these experiments, an ultrashort laser pulse is split into two portions: one of the pulses (pump) is used to inject nonequilibrium excitations and the other pulse (probe) is used to probe the subsequent temporal evolution of the density of these excitations via measurement of the change in reflectivity of the sample, assumed proportional to the QP population n, as a function of time. These experiments have been performed in the cuprates [11,12,15] to study fundamental issues of gap symmetry and recombination dynamics, and have recently been applied to the pnictides to provide evidence for a psuedogap state [13] and the existence of competing electronic order [14]. However, ultrafast studies of QP recombination dynamics which can reveal the structure of the superconducting energy gap in momentum space have not been previously investigated.

In this Letter, we present an optical pump-probe study of QP recombination in $Ba_{0.6}K_{0.4}Fe_2As_2$ ($T_c = 37$ K) that reveals band-specific dynamics. Below T_c, we find that our signal is comprised of two distinct components which, aided by LDA calculations [16] and ARPES measurements [1,17–19], we assign to the three Fermi surface hole pockets. The first component, which we assign to the innermost hole pockets, is characterized by a fast QP decay rate, which depends linearly on the excitation density, signifying pairwise recombination. By studying the excitation density dependence of this decay, we obtained the thermal recombination rate of QPs, which was found to vary as $\sim T^2$. The second component is a slow, excitation density independent decay indicative of "bottlenecked" recombination of QPs from a different component of the superconducting system, which we assign to the outer hole band. The number of photoinduced QPs (n) contributing to the overall signal increases linearly with laser fluence, indicat-

ing the fully gapped character of these bands. These observations are consistent with models which predict fully gapped hole bands and nodal or very anisotropic gaps in the electron pockets.

For this study, we used a Ti:sapphire oscillator producing pulses with center wavelength 795 nm ($h\nu = 1.56$ eV) and duration 60 fs at FWHM. The 80 MHz repetition rate was reduced to 1.6 MHz with a pulse picker to eliminate steady state heating of the sample. Both beams were focused to 60 μm FWHM spots and the probe beam reflected back to a photodiode for detection. Use of a double-modulation scheme [11] provided sensitivity of the fractional change in reflectivity of $\Delta R/R \sim 10^{-7}$. The pump fluence Φ was varied with neutral density filters in order to tune the QP excitation density. High-quality single crystals of $Ba_{0.6}K_{0.4}Fe_2As_2$ were grown by the self-flux method [20]. SQUID magnetometry measurements yielded a very sharp transition ($\Delta T \approx 1$ K) at $T_c = 37$ K indicating a high degree of sample purity.

Figures 1(a) and 1(b) show raw data traces of $\Delta R(t)/R$ normalized to their $t = 0$ value at 7 and 60 K, respectively, for a variety of Φ. At 7 K, photoexcitation leads to a decrease in the reflectivity and the rate of recovery increases with increasing pump fluence. At 60 K, we observe data collapse of the normalized traces indicating that all $T > T_c$ recovery dynamics are independent of Φ. From the data in Figs. 1(a) and 1(b), we conclude that the decay rate at short times increases both with increasing temperature and excitation density below T_c. In order to rule out steady state heating as the source of this intensity dependence, we used a pulse picker to vary the repetition rate from 1.6 MHz to 200 kHz, which produced no discernible change in the recovery dynamics.

Closer examination of the data in Fig. 1(a) reveals that after the initial intensity-dependent relaxation, $\Delta R(t)/R$ tends to a constant offset of $(\Delta R/R)_{norm} \simeq 0.5$. This offset is the beginning a slow component in the signal, shown in Fig. 2(a), whose decay was observed to be intensity independent. As with the fast intensity dependence, the slow component was observed to switch off abruptly at T_c, signifying its origin in superconductivity [Fig. 2(b)].
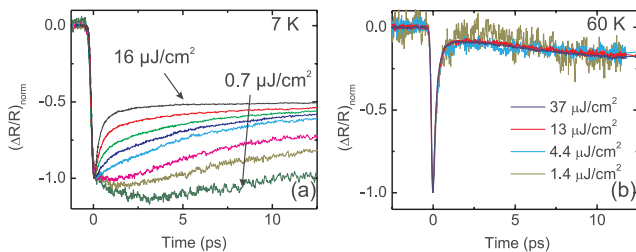
The characteristics of these two separate relaxation time scales can be understood by considering the coupled dynamics of gap energy QPs and bosons within the context of the Rothwarf-Taylor (RT) model [21]. In this model, there are three important rates that determine the behavior of the system [11,22], each depicted schematically in Fig. 3(a). The first is the bare recombination rate of QPs in which two QPs form a Cooper pair and emit a 2Δ boson. This rate goes as $\gamma_r = -\frac{1}{n}\frac{dn}{dt}$ and depends linearly on the population n ($\gamma_r = Bn$, where B is the bimolecular recombination coefficient). The emitted boson can then either recreate the QP pair with rate γ_{pc} or escape with rate γ_{esc}. This escape ultimately occurs either via decay into other, lower energy ($<2\Delta$) bosons or by propagation out of the probed region. The relative magnitudes of these three rates determines if the density-dependent bare QP recombination rate can be observed.

The fast component observed in Fig. 1(a) is analyzed by obtaining the initial slope of the transients following the peak. This initial decay rate (γ_{r0}) exhibits bare QP recombination, as evidenced by its linear increase with excitation density at low fluences, shown by the black squares in Fig. 3(b). The observation of bimolecular recombination physically originates from either a very slow pair creation rate ($\gamma_{pc}/Bn \ll 1$) or a very fast escape rate such that the pairing boson escapes before it has a chance to break apart a Cooper pair ($\gamma_{esc} \gg \gamma_{pc}$) [10].

In turn, the slow component of Fig. 2(a) reflects a separate set of dynamics. While prior studies in the cuprates have suggested that laser heating [23] or QPs trapped in in-gap states [24] may cause a slow decay, the decay observed here does not fit within either of these proposed scenarios. The former is precluded by the sudden disappearance of the slow component at T_c while the latter is ruled out due to the consistency of the slow component between different sample batches, where variability in impurity concentration would cause marked differences.
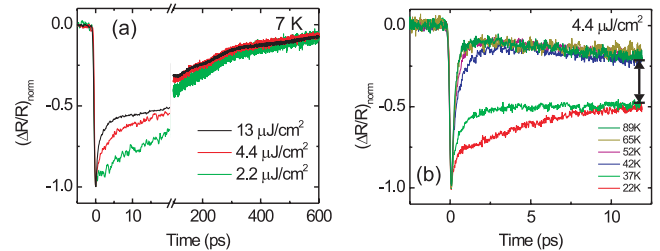

FIG. 2 (color).   Slow relaxation of $(\Delta R/R)_{norm}$ in the superconducting state. (a) $(\Delta R/R)_{norm}$ at 7 K measured at three different fluences show no intensity dependence in the slow dynamics despite their marked intensity dependence at short times. (b) Temperature dependence of $(\Delta R/R)_{norm}$ near T_c obtained at $\Phi = 4.4$ J/cm^2. We note a sharp decrease in the offset across the transition (i.e., 37 to 42 K) due to switching off of the long-time component with loss of superconductivity. Above T_c there is an upturn of the signal evident at short times due to stimulated Brillouin scattering [27].

FIG. 1 (color).   Fast, intensity-dependent relaxation of the normalized reflectivity transients $(\Delta R/R)_{norm}$ in the superconducting state. The decay rate of $(\Delta R(t)/R)_{norm}$ systematically decreases with decreasing intensity at 7 K (a) [from bottom to top: $\Phi = 0.7$ μJ/cm^2 (light green), 2.2, 4.4, 7.0, 8.9, 12.8 to 16.1 μJ/cm^2 (black)] but not at 60 K (b).

Rather, we ascribe these dynamics to a separate QP recombination process governed by a different set of RT parameters where γ_{esc} is the slowest, i.e., $\gamma_{esc} \ll \gamma_{pc}, Bn$. Here, one observes the boson bottleneck in which QPs and bosons quickly come to a quasiequilibrium [22] and the combined population finally decays with a slow, intensity independent rate proportional to γ_{esc}.

We may thus exploit the distinctive relaxation dynamics of the fast component to obtain clues about the symmetry and structure of the superconducting gap [11] via the thermal decay rate of QPs participating in recombination. In the low excitation regime, the thermal density of QPs (n_{th}) becomes comparable with the photoinduced QP density. A photoinduced QP can then either recombine with another photoinduced QP or a thermally excited QP, resulting in an aggregate decay rate $\gamma_{r0} = Bn + 2Bn_{th}$. Figure 3(b) shows γ_{r0} as a function of laser fluence (Φ) for four representative temperatures. We observe that at each temperature, γ_{r0} increases linearly in Φ with a temperature dependent intercept. This linear dependence is due to the first term in γ_{r0} (Bn) and the intercept is the thermal recombination rate ($2\gamma_{th} = 2Bn_{th}$ as $n \propto \Phi \to 0$). The slope of the linear fits (B) exhibits no strong temperature dependence while the intercept $2Bn_{th}$ increases with T due to a larger n_{th}.

Figure 3(c) presents the temperature dependence of γ_{th} and γ_{r0} at various fluences, both in the high and low fluence regimes. The signature of pairwise recombination is evident through the strong dependence of γ_{r0} on the excitation density, which diminishes markedly at T_c. Significantly, we note that the thermal decay rate depends quadratically on temperature ($\gamma_{th} = Bn_{th} \propto T^2$) below T_c. In the case of a simple isotropic s-wave gap, n_{th} is expected to depend on T as $\sim \exp(-\Delta/k_bT)$, whereas the presence of a node would give rise to a power law dependence. In particular, a line node in the gap would lead to the observed $n_{th} \propto T^2$ due to the linear dependence of the density of states on energy in the node.

A significant piece of information regarding the possible location of such a node in momentum space is provided by consideration of the dependence of the photoinduced QP density (n) on the total energy deposited into the system. As mentioned above, the amplitude of the measured change in reflectivity is proportional to n, whereas the absorbed laser fluence (Φ) is proportional to the total energy stored in the QP system. For fully gapped excitations, n is proportional to the total energy absorbed, and hence we simply have $\Delta R/R \propto \Phi$ [11]. In the presence of a line node, the linear dependence of the density of states on energy implies that n should vary with the total stored energy in a sublinear fashion ($\Delta R/R \propto \Phi^{2/3}$) [11]. Figure 3(d) shows the amplitude of $\Delta R/R$ as a function of Φ at low fluence for four temperatures, where a clear linear dependence is observed at all temperatures, indicating that the photoinduced QPs all originate from fully gapped excitations.

The simultaneous observation of nodal (i.e., $n_{th} \propto T^2$) and fully gapped (i.e. $n \propto \Phi$) characteristics in our data may be traced to the multiband nature of pnictides. ARPES measurements have shown that five bands cross the Fermi surface: three hole bands near zone center (Γ) and two at zone edge (M) [Fig. 4(a)]. We attribute the entirety of the observed signal to the three hole pockets at Γ, (i.e., the inner hole bands α and outer hole band β, using the nomenclature of [17]). Neither of the electron bands at M (γ and δ) contribute significantly to the signal as LDA calculations [16] reveal a dearth of accessible states 1.5 eV above and (properly renormalized [19]) below the Fermi level at this point in the Brillouin zone, rendering QP recombination there optically dark at our probe wavelength. Furthermore, an estimate of the Sommerfeld parameter shows that the density of states at β and at the combination of the two bands at α are each 7 times larger than at γ and δ [17], with the implication that the number of photoinduced QPs in the hole pockets should overwhelm that of the electron pockets.

The band structure and possible QP relaxation channels allow assignment of the fast dynamics to the α band and the slow component to β. The observation of a dispersion kink in ARPES measurements at 25 meV that appears in α and γ, δ but not β [18,19] indicates a strong coupling between α and γ, δ by an excitation at 13 meV, interpreted to be a resonant magnetic excitation [25], and which arises
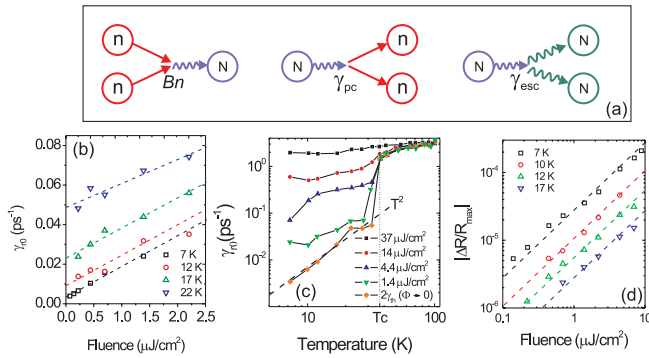

FIG. 3 (color).   Decay-rate analysis of data with a view towards gap symmetry. (a) Illustration of the three rates in the Rothwarf-Taylor model: Bare QP recombination rate (Bn), pair creation rate (γ_{pc}), and escape rate (γ_{esc}). (n: QP, N: Bosons) (b) The initial decay rate (γ_{r0}) as a function of pump fluence at various temperatures. The linear dependence of the recombination rate on initial population is a hallmark of bimolecular recombination. Dashed lines show linear fits to data. The thermal decay rate at each temperature was obtained by extrapolating the fits to zero fluence. (c) The initial relaxation rate γ_{r0} plotted as a function of temperature for five representative pump fluences along with the thermal rate γ_{th} (orange diamonds). Below T_c, γ_{r0} strongly depends on the excitation density. There is a sharp transition at 37 K, although a discernible intensity dependence persists above T_c. The dashed line shows $\sim T^2$ dependence as a guide. (d) $|(\Delta R/R)_{max}|$ plotted as a function of Φ for four temperatures, each offset for clarity. Dashed lines show a slope of 1.
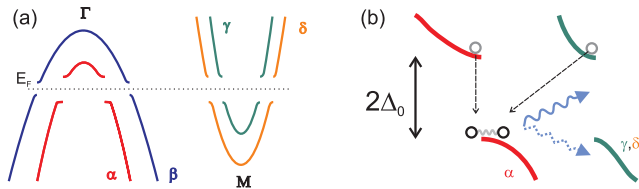
FIG. 4 (color). (a) Schematic representation of the electron and hole bands crossing the Fermi level in the superconducting state. (b) Interband recombination of QPs in the α bands can occur with their counterparts in the electron bands. As a result, a Cooper pair, an optical phonon and an antiferromagnetic spin fluctuation are produced.

due to their near-perfect Fermi surface nesting. This excitation makes it possible for the QPs in α to pair up with their counterparts in γ, δ through an interband process by emitting a combination of an optical phonon and a magnetic excitation [Fig. 4(b)]. The inverse process, however, is necessarily very slow since three-body scattering of an antiferromagnetic spin fluctuation, an optical phonon and a Cooper pair is required to generate QPs. The short lifetime of the magnetic mode, as indicated by its relatively broad energy linewidth [25], further inhibits the reverse process, leading to a small value of γ_{pc} which prevents formation of a bottleneck in the interband channel. In the case of intraband recombination in α, which occurs by emission of an A_{1g} optical phonon ($E = 2\Delta_0 = 24$ meV), its short lifetime (3 ps) [26] precludes it, too, from generating a bottleneck. We therefore ascribe the intensity-dependent decay to bare QP recombination in α and the slow dynamics to a boson bottleneck in β. This bottleneck is enhanced by the difference in gap energies between α ($2\Delta = 24$ meV) and β ($2\Delta = 12$ meV), since, in addition to the bosons already present from intraband recombination in β, single bosons emitted from the interband recombination between α and γ, δ may also break pairs in β.

These assignments allow for a proper interpretation of the simultaneous observation of $n_{th} \propto T^2$ and $\Delta R/R \propto \Phi$. The thermal QPs participating in the observed recombination at low fluences are not necessarily the same as the photoinduced ones; rather, they may also originate from either γ or δ. A line node in either γ or δ will lead to a preponderance of thermally excited QPs from the electron bands as compared with the fully gapped hole bands. These QPs will then dominate the recombination process which, in tandem with the interband recombination process described above, can account for the observed behavior in its entirety. While another possibility for the quadratic temperature dependence of n_{th} is the proposed $s_{\pm}$ gap symmetry with interband impurity scattering, this scenario can only be realized within a very specific range of impurity parameters [3]. Therefore, while we cannot definitively differentiate between the two scenarios at present, our results are highly suggestive of nodes in the electron pockets.

In summary, we have presented time resolved measurements of band-dependent QP dynamics in $Ba_{0.6}K_{0.4}Fe_2As_2$. Below T_c, we find that the rate of QP recombination increases linearly with excitation density indicating pairwise recombination within the inner hole band. The number of photoinduced QPs increases linearly with excitation density indicating fully gapped nature of the hole bands. Meanwhile, the dynamics within the outer hole band exhibit bottlenecked recombination. We have observed that the thermal recombination rate of QPs varies as T^2. This likely arises from a line node in the electron bands although we cannot definitively rule out the $s_{\pm}$ order parameter with interband impurity scattering at this time.

*gedik@mit.edu
[1] H. Ding et al., Europhys. Lett. **83**, 47001 (2008).
[2] I. I. Mazin et al., Phys. Rev. Lett. **101**, 057003 (2008).
[3] A. V. Chubukov, D. V. Efremov, and I. Eremin, Phys. Rev. B **78**, 134512 (2008).
[4] H. Fukazawa et al., J. Phys. Soc. Jpn. **78**, 033704 (2009).
[5] C. Martin et al., Phys. Rev. B **80**, 020501 (2009).
[6] S. Graser et al., New J. Phys. **11**, 025016 (2009).
[7] Y. Yanagi, Y. Yamakawa, and Y. Ono, J. Phys. Soc. Jpn. **77**, 123701 (2008).
[8] A. V. Chubukov, M. G. Vavilov, and A. B. Vorontsov, Phys. Rev. B **80**, 140515 (2009).
[9] R. D. Averitt and A. J. Taylor, J. Phys. Condens. Matter **14**, R1357 (2002).
[10] G. P. Segre et al., Phys. Rev. Lett. **88**, 137001 (2002).
[11] N. Gedik et al., Phys. Rev. B **70**, 014504 (2004).
[12] N. Gedik et al., Phys. Rev. Lett. **95**, 117005 (2005).
[13] T. Mertelj et al., Phys. Rev. Lett. **102**, 117002 (2009).
[14] E. E. M. Chia et al., Phys. Rev. Lett. **104**, 027003 (2010).
[15] J. Demsar et al., Phys. Rev. Lett. **91**, 267002 (2003).
[16] F. Ma, Z.-Y. Lu, and T. Xiang, Front. Phys. China, **5**, 150 (2010).
[17] H. Ding et al., arXiv:0812.0534.
[18] P. Richard et al., Phys. Rev. Lett. **102**, 047003 (2009).
[19] L. Wray et al., Phys. Rev. B **78**, 184508 (2008).
[20] G. F. Chen et al., Phys. Rev. B **78**, 224512 (2008).
[21] A. Rothwarf and B. N. Taylor, Phys. Rev. Lett. **19**, 27 (1967).
[22] V. V. Kabanov, J. Demsar, and D. Mihailovic, Phys. Rev. Lett. **95**, 147002 (2005).
[23] I. I. Mazin, Phys. Rev. Lett. **80**, 3664 (1998).
[24] T. N. Thomas et al., Phys. Rev. B **53**, 12436 (1996).
[25] A. D. Christianson et al., Nature (London) **456**, 930 (2008).
[26] B. Mansart et al., Phys. Rev. B **80**, 172504 (2009).
[27] C. Thomsen et al., Phys. Rev. B **34**, 4129 (1986).